# Structural features of spin-coated thin films of binary $As_xS_{100-x}$ chalcogenide glass system

J. Cook<sup>1</sup>, S. Slang<sup>2</sup>, R. Golovchak<sup>1</sup>, H. Jain<sup>3</sup>, M. Vlcek<sup>2</sup>, A. Kovalskiy<sup>1,\*</sup>

Austin Peay State University, Clarksville, TN, 37075, USA
Faculty of Chemical Technology, University of Pardubice, 53210 Pardubice, Czech Republic
International Materials Institute for New Functionality in Glass, Lehigh University, Bethlehem, PA, 18015

#### **Abstract**

Spin-coating technology offers a convenient method for fabricating photostable chalcogenide glass thin films that are especially attractive for applications in IR optics. In this paper we report the structure of spin-coated  $As_xS_{100-x}$  (x = 30, 35, 40) thin films as determined using high resolution x-ray photoelectron spectroscopy (XPS) and Raman spectroscopy, especially in relation to composition (i.e. As/S ratio) and preparation process variables. It was observed that As atoms during preparation have a tendency to precipitate out in close to stoichiometric compositions. The mechanism of bonding between the inorganic matrix and organic residuals is discussed based on the experimental data. A weak interaction between S ions and amine-based clusters is proposed as the basis of structural organization of the organic-inorganic interface.

#### Introduction

Chalcogenide glasses (ChG) are attractive materials for a variety of applications, most notably in IR optics due to their high refractive indices, wide IR transmission window, and high optical nonlinearities [1-6]. Some ChG applications (i.e. diffraction gratings, waveguides etc.) require the material to be in thin film form [4,5,7-12]. Current standard methods for thin film deposition of ChG include thermal evaporation, sputtering, pulsed laser deposition and spin-coating [13,14]. While thermal evaporation is known to produce optical quality thin films with a well-studied structure, it is technologically challenging and requires the use of high vacuum [3,15]. In addition, the resulting films are highly photosensitive in UV-VIS spectral range, which is undesirable for most IR devices [3,15]. Spin-coating is an attractive alternative to thermal deposition, offering the possibility of manufacturing of large-area films with a structure closer to that of the bulk glass. It does not require the use of high vacuum, and has the capability to produce high quality thin films at a much lower cost and more quickly than ones produced by thermal deposition. Moreover, photoinduced changes of optical transmission under band-gap light of moderate intensity (for example, 10 mW He-Ne 633 nm laser) were observed only for chalcogen-deficient AsSe spincoated films (SCF) [16]. By comparison, SCF of stoichiometric or chalcogen-rich ChG compositions are expected to be much less sensitive to light irradiation, maintaining the structure of bulk chalcogenide glass. The only report on the photosensitivity of such SCF was for  $As_{40}S_{60}$ with 250 W tungsten-mercury lamp high intensity, super-bandgap light [16]. Notwithstanding, the main obstacle preventing a widespread adoption of the ChG-based SCF for IR applications is the existence of organic residuals within the glass matrix. These residuals are responsible for the undesirable modification of the structural and optical properties of these thin films.

E-mail address: kovalskyya@apsu.edu

<sup>\*</sup> Corresponding author.

To make SCF more technologically relevant, it is important to minimize the influence of residuals on optical properties, especially in the near IR region. A detailed structural characterization is necessary in order to determine the influence of organic solvent on the structure of glass matrix. However, present knowledge on the structure of SCF is quite limited. Chern and Lauks studied binary SCF using a combination of NMR, IR spectroscopy and thermal analysis techniques [17-20], but other advanced methods such as high resolution X-ray Photoelectron Spectroscopy (XPS) and Raman spectroscopy have not been employed for a comprehensive understanding of their structure.

XPS has been successfully exploited to determine the structure of a broad range of binary and ternary chalcogenide glass systems, including As-S, As-Se, Ge-S, Ge-Se, As-Ge-Se etc., including the chemical environments of the constituent elements [21-24]. It has been used primarily to investigate the structure of thermally evaporated ChG thin films [8,25-27], while such structural information is not available for SCFs. Therefore, in the present study we focus on the binary  $As_xS_{100-x}$  SCFs as a model ChG system. The goal is to combine the XPS data with Raman spectroscopy results to provide relevant structural information. This combination delivers data on both the bulk and surface structure of the thin films.

### **Experimental**

Bulk  $As_xS_{100-x}$  glasses (x=30, 35, 40) prepared by the standard melt quench technique were used as the starting material for fabricating SCF. The bulk glass were prepared starting with high purity (5N) elemental powders forming approximately 10 g batch, which was loaded into quartz ampoules and vacuum sealed. The ampoules were then heated to 900° C in a rocking furnace for 24 hours to homogenize the melt, which was then quenched in cold water to solidify the melt and form glass.

To spin-coat thin films, bulk glass was first dissolved in a suitable solvent, in this case n-propylamine or n-butylamine in different concentrations in order to yield the desired film thickness. After dissolution, the chalcogenide solution was pipetted onto microscope slides rotating inside a Smart Coater SC100 spin-coater. The substrate rotation speed was adjusted to match specific requirements for the given composition of glass being deposited. After deposition, films were transferred immediately to a hot plate to anneal at 60°C for 20 min in air and the obtained samples were subsequently stored in a dry, dark environment.

To examine the effects of light and temperature on the structure of SCF,  $As_{35}S_{65}$  films were also thermally annealed for 60 minutes at  $100^{\circ}$  C in an argon atmosphere and exposed to a halogen lamp for 60 minutes in the same conditions. This composition was chosen due to the good quality of films produced as well as to relatively small loss of As due to precipitation during solution preparation.

Light from LEDs with wavelengths close to band gap energy and power  $\sim 100$  mW was used to irradiate  $As_{30}S_{70}$  and  $As_{40}S_{60}$  SCF for 60 minutes in argon atmosphere to estimate the level of photoinduced optical effects in S-rich and stoichiometric films. Transmission spectra in the range 300-3000 cm<sup>-1</sup> were recorded for the SCF before and after irradiation using a Shimadzu UV-3600 spectrophotometer. Films were thick enough to provide accurate data on the optical absorption edge, and a specific alignment procedure was used to ensure the spectra were measured at the same spot the film was irradiated.

For obtaining Raman spectra spin-coated thin films were scraped off of substrates and packed into aluminum holders. Then the spectra were recorded using an excitation laser beam with

 $\lambda = 1064$  nm, and output power of 50 mW (IFS55/FRA106, Bruker FT Raman spectrometer). Measurement resolution was 2 cm<sup>-1</sup> and 200 scans were recorded for each sample.

High-resolution XPS spectra were recorded with a Scienta ESCA-300 spectrometer using monochromatic Al  $K_{\alpha}$  X-rays (1486.6 eV) under a vacuum of 2 x  $10^{-8}$  Torr or better. For all measurements the angle between the surface and the detector was  $90^{\circ}$ . The instrument was operated in a mode that yielded a Fermi level width of 0.4 eV for Ag metal and at a full width at half maximum (FWHM) of 0.54 eV for Ag  $3d_{5/2}$  core level peak. The energy scale was calibrated using the Fermi level of clean Ag. The XPS data consisted of selected scans over the core level peaks of interest. An energy increment of 0.05 eV was used for measuring the core level spectra. The core level peaks were recorded using the constant pass energy of 150 eV. The surface charging from photoelectron emission was neutralized using a low energy (< 10 eV) electron flood gun.

Data analysis was conducted with the standard CASA-XPS software package. For analyzing the core level spectra, Shirley background was subtracted and a Voigt line shape was assumed for the peaks [28]. The 3d core level XPS spectra of As and 2p core level spectra of S were used for quantitative analysis of chemical environment in the investigated samples. The number of doublets within a given peak was determined by an iterative curve fitting procedure in which a doublet was added only if it significantly improved the goodness of the fit of the experimental data to the envelope of the fitted curve. The parameters used to link the As  $3d_{5/2}$  and  $3d_{3/2}$  peaks were: a peak separation of 0.68 eV and an area ratio of 1.4. For the S  $2p_{3/2}$  and  $2p_{1/2}$  peaks of S 2p core level the parameters were 1.16 eV and 2.0, respectively. The FWHM was assumed to be the same for the peaks within one doublet. However, differences between FWHM values for different doublets of the same core-level peak were allowed. The mix between the Gaussian and Lorentzian fractions in the Voigt function was chosen to be the same for all doublets of a given core level. With these constraints the uncertainty in the peak position (BE) and area (A) of each component was  $\pm 0.05$  eV and  $\pm 2\%$ , respectively.

#### **Results**

The S 2p and As 3d core level XPS spectra were measured for the SCF of three glass compositions  $As_{30}S_{70}$ ,  $As_{35}S_{65}$  and  $As_{40}S_{60}$ . Fitting parameters such as FWHM, area, and positions for all peaks are presented in Table 1. Chemical composition of the films was determined from the areas under the core level XPS spectra and appropriate sensitivity factors.

All  $As\ 3d$  spectra were successfully fitted by one doublet representing the spin-orbit splitting of the d level electrons. For all  $As\ 3d$  spectra, as shown in Figure 1, the binding energy of the  $3d_{5/2}$  peak component is found to be  $43.10 \pm 0.10$  eV.

The compositional dependence of S 2p core level electron spectra is presented in Figure 2. For all three compositions, there are three main contributions of S atoms to the structure, each represented by an appropriate doublet in the fit. The  $2p_{3/2}$  component of the Peak 1 doublet is located at 162.10-162.30 eV, the same components for the Peak 2 and Peak 3 are located at 162.90-163.10 eV and 161.00-161.20 eV, respectively (Table 1). In the S-rich  $As_{30}S_{70}$  and  $As_{35}S_{65}$  compositions, a new doublet, Peak 4, emerges with main component at 163.70 eV, which indicates an additional environment with higher electronegativity around S atoms. A number of differences are observed in the peaks' intensities and areas with change in composition of the films. A strong increase in the intensity of Peak 1 and decrease in the intensity of Peak 2 are observed with increasing As content. On the other hand, the area of Peak 3 in all three compositions is approximately the same at the level of  $\sim$ 9-10%.

XPS core level spectra were also measured for thermally annealed and light exposed SCF of  $As_{35}S_{65}$  composition. The respective  $As_{3d}$  and  $S_{2p}$  XPS spectra are shown in Figures 3 and 4. Film compositions and XPS fitting parameters for both  $As_{3d}$  and  $S_{2p}$  spectra are also presented in Table 1. The  $As_{3d}$  core level XPS spectra of the annealed and exposed SCF consist of only one doublet. Therefore, with a high confidence it can be attributed to  $As_{3d/2}$  pyramids in both cases, with the main  $3d_{5/2}$  component located at ~43.1 eV [29]. The relative difference between the position of  $As_{3d/2}$  and  $S_{2p/3/2}$  associated with S in pyramidal units in virgin, annealed and exposed samples is identical, providing an additional argument for the above assignment.

All S2p XPS spectra of annealed and exposed SCF consist of three doublets indicating three distinct chemical configurations of S atoms, having their binding energies for main components at  $\sim 162.3$  eV (Peak 1),  $\sim 163.1$  eV (Peak 2),  $\sim 161.2$  eV (Peak 3) and  $\sim 163.7$  eV (Peak 4). It is observed that exposure with halogen lamp has a dramatic impact on the concentrations of individual chemical environments, causing a  $\sim 7\%$  decrease in Peak 1 area, a  $\sim 16\%$  increase in Peak 2 area and  $\sim 7\%$  decrease in Peak 3 area with respect to virgin SCF. On the other hand, annealing is found to have a much smaller effect on the overall structure of SC layers.

Optical spectroscopy in the vicinity of fundamental optical absorption edge region shows absence of any photoinduced optical changes caused by bandgap light in SCF (Figure 5). To prove this behavior, we have chosen both *S*-rich  $As_{30}S_{70}$  and As-rich  $As_{40}S_{60}$  compositions.

The volume structure of the virgin (preliminary heat treatment at  $60^{\circ}$ C) and annealed (at  $100^{\circ}$ C) thin films of  $As_{30}S_{70}$  glass composition was determined by Raman spectroscopy. Two main bands at  $342 \text{ cm}^{-1}$  and  $369 \text{ cm}^{-1}$  and less intense peaks at  $151 \text{ cm}^{-1}$ ,  $218 \text{ cm}^{-1}$ ,  $475 \text{ cm}^{-1}$  and  $495 \text{ cm}^{-1}$  are observed in the Raman spectra of these films (Figure 6). Noticeable also is a wide band at  $2800\text{-}3000 \text{ cm}^{-1}$ . Annealing causes a decrease in the intensity of the bands at  $\sim 230 \text{ cm}^{-1}$ ,  $415 \text{ cm}^{-1}$  and  $2800\text{-}3000 \text{ cm}^{-1}$ . Additionally, the chemical structure of the precipitate of  $As_{35}S_{65}$  solution was studied as shown in Figure 7. Strong bands are observed at  $85 \text{ cm}^{-1}$ ,  $268 \text{ cm}^{-1}$  and  $369 \text{ cm}^{-1}$  while less intense bands are also visible at  $183 \text{ cm}^{-1}$ ,  $471 \text{ cm}^{-1}$  and  $561 \text{ cm}^{-1}$ .

#### **Discussion**

XPS is uniquely suited to provide the chemical composition of the surface layer (~10 nm) of materials under consideration. It is deep enough to infer structural information and observe general trends in the composition of the thin films.

In the case of  $As_{35}S_{65}$  and  $As_{40}S_{60}$  samples, there is a major change in the composition of the resulting SCF compared with the bulk glass used to deposit them. However, for  $As_{30}S_{70}$  SCF, there is no significant change in the As/S ratio, compared to that of the bulk glass. As the arsenic content increases, we see the composition of the resulting film deviates away from the expected chemical makeup. For  $As_{35}S_{65}$ , the composition was measured roughly  $As_{32}S_{68}$  and the As/S ratio for stoichiometric  $As_{40}S_{60}$  films was 35/65, indicating a loss of As in both cases.

One of the predominant mechanisms responsible for this loss of As is its precipitation during the dissolution of ChG in solvent. Increasing As content in bulk glass directly leads to a higher volume of precipitate in the resulting spin-coating solution and thus a higher quantity of As lost. However, we cannot exclude that this As deficiency is also related to the loss of As due to evaporation of As-amine compounds during the annealing stage. This decrease of As concentration should be more efficient from the surface layer of SCF and could create the observed gradient of As concentration. Based on the volume of precipitate produced during dissolution of bulk glass, evaporation of As and As-containing compounds is expected to play a much smaller role in the loss of As and the resultant concentration profile than does precipitation.

As 3d XPS core level spectra, shown in Figure 1, for all three compositions  $As_{30}S_{70}$ ,  $As_{35}S_{65}$  and  $As_{40}S_{60}$  of SCF indicate the presence of only one chemical environment around As atoms. The position of As  $3d_{5/2}$  peak at  $\sim$ 43.1 eV is attributed to S-As< $(S)_2$  (target atom in bold) pyramidal units traditionally associated with bulk As-S glasses [24]. The As XPS spectrum of SCF fundamentally differs from those produced by thermal evaporation. Whereas there is one chemical configuration involving As atoms in SCF, thermally deposited layers usually have two As environments, corresponding to  $AsS_{3/2}$  pyramids at  $\sim$ 43.0 eV and units containing As-As homopolar bonds at lower BE [25]. The content of vapor produced during thermal evaporation includes a variety of molecular species containing homopolar bonds including As-rich  $As_4S_4$  and  $As_4S_3$ . These vapors condense very quickly on the substrate at room temperature and are frozen into the structure of evaporated films [30]. The position of the peaks corresponding to As-rich compounds containing As-As bonds is determined by the lower electronegativity of As compared with S. As we see only As in  $AsS_{3/2}$  units in spin-coated films, the lack of homopolar bonds indicates that either As-As bonds are not present in the surface layer of these samples or their concentration is below the reliable sensitivity limit of the XPS technique, approximately 2 at.%.

S 2p XPS core level spectra for  $As_{30}S_{70}$ ,  $As_{35}S_{65}$  and  $As_{40}S_{60}$  SCF, presented in Figure 2, show the existence of three doublets in all three samples. Peak 1 with S 2 $p_{3/2}$  component at ~162.1 eV is attributed to As-S-As fragments connecting the  $AsS_3$  pyramidal units [24], Peak 2 with main component at ~163.0 eV is related to S-S-As fragments and Peak 3 with main component at ~161.0 eV is assigned to a single-coordinated sulfur, which can be associated, for example, with dangling bonds or non-bridging sulfur [3]. The latter peak can also originate from S- ions proposed in the vicinity of solvent's — $NH_2$  complexes throughout the SCF network by Chern and Lauks [18]. According to their results, the S- ions can be formed during dissolution of bulk glass as nitrogen lone pair donor electrons are transferred to As atoms and break As-S bonds, forming S- ions and As-amine complexes. These S- ions are very weakly ionically bonded to — $NH_3$ + which is responsible for the lower BE of this S environment [18]. The additional peak 4 is present only in the S-rich  $As_{30}S_{70}$  and  $As_{35}S_{65}$  compositions and has been assigned to S-S-S fragments [24]. The position of this peak at higher BE is associated with the higher electronegativity of S atoms in comparison with As.

The mentioned formation of  $S^-$  ions and As-amine complexes should result also in additional component(s) within the analysis of As 3d core level peak. However, our XPS spectra did not reveal any features related to such chemical environment of As. This point is discussed below in the context of Raman spectra analysis.

It is observed also that the concentrations of structural units linked with Peak 1 and Peak 2 in S2p core level XPS spectra are dependent upon the As content of bulk glasses. With increasing As content, the intensity of Peak 1 associated with pyramids increases, while Peak 2 simultaneously decreases. The trade-off between Peak 1 and Peak 2 indicates that the As-S-As structural unit become more prevalent than S-S-As, which is expected with the increase in As content when the As atoms replace S atoms within the glass network. Additionally, a dependence variation of the FWHM for each S2p spectra with glass composition is noticed. The S2p spectrum for  $As_{30}S_{70}$  has the largest FWHM compared with other compositions. With an increase in the As content, the total FWHM of S2p spectra decreases from 2.15 eV to 1.90 eV to 1.74 eV for  $As_{30}S_{70}$ ,  $As_{35}S_{65}$  and  $As_{40}S_{60}$ , respectively. The accompanying relative increase in the intensity of Peak 1 indicates less variation in the chemical environment of S atoms and is responsible for the corresponding decrease of the FWHM.

In addition to the compositional analysis, the structure of  $As_{35}S_{65}$  SCF was studied after annealing and exposure, which are the usual stimuli, leading to the additional release of residual organic solvent. Structural studies after these treatments are of special importance in order to understand their effects on the structure of SCF. The  $As_{3d}$  core level XPS spectra shown in Figure 3 do not reveal any significant changes, indicating that light and temperature do not cause noticeable structural transformations associated with  $As_{3d}$  atoms in the SCF.

The S 2p core level XPS spectra for the same samples in Figure 4 show three environments for each of them. Peak assignments are the same as those described above, where Peak 1 corresponds to As-S-As fragments, Peak 2 to S-S-As units, Peak 3 to single-coordinated sulfur and Peak 4 to S-S-S. After annealing, it is observed that the concentration of Peak 1 increases while Peak 2 simultaneously decreases. This trend indicates a loss of S atoms and relative increase in As atoms (compare the actual compositions of the annealed and virgin samples in Table 1), which is probably caused by the release of S atoms together with organic residual during annealing.

The exposure to halogen lamp radiation has a pronounced effect on the organization of S bonds within the surface layers of SCF. The Peak 1 and Peak 3 decrease each by  $\sim$ 7%, while Peak 2 increases from  $\sim$ 21% to  $\sim$ 37%, indicating an increase of *S-S-As* units. This transformation causes the structure of the films to become more similar to that of bulk glass. The fraction of each chemical environment becomes closer to the distribution of S bonds in bulk *As-S* glass of corresponding composition [24,27]. The most likely phenomenon responsible for the rearrangement of *S* bonds is photostructural transformation caused by the UV part of the halogen light spectrum [16] and photoinduced release of organic residual. Upon irradiation, a part of singly bonded *S* ions, previously involved in the creation of organic-inorganic interface, participate in the formation of *S-S-As* structural units which are more stable than the ionic configuration.

It is important to note that neither the As 3d nor the S 2p XPS core level spectra suggest the presence of any As-C, As-N, S-C or S-N bonds. The lack of these bonds indicates that no organic solvent or organic material is directly bonded within the glass network. This fact is an additional confirmation of the structural model put forward by Chern and Lauks described elsewhere [17,18].

Our experiments show that the optical gap of SCF is not sensitive to exposure to bandgap radiation (Fig. 5), which is contrary to thermally evaporated thin films that are extremely photosensitive due to the presence of a large number of "wrong" homopolar bonds frozen into the thin film matrix during deposition. We believe that the lack of these homopolar *As-As* bonds in SCF is the structural reason for their photostability. So, the changes observed by XPS in the exposed SCF could not be related to the *As-S* bonds switching and accompanied topological defects formation (responsible for the photodarkening effect in thermally-evaporated thin films) under the bandgap light irradiation. These changes can be attributed to structural transformations mostly in the surface layers caused by UV light present in halogen lamp spectrum [5].

The bulk structure of virgin and annealed thin films of  $As_{30}S_{70}$  glass composition was determined by Raman spectroscopy. Seen in Figure 6, the strong band at 342 cm<sup>-1</sup> confirms, that the basic structural unit of studied thin layers is trigonal pyramid  $AsS_{3/2}$  [31-34]. The presence of the shoulder at 369 cm<sup>-1</sup> proves that deeper layers also contain realgar-like structural units of  $As_4S_4$  [33,35]. The strong bands at 151, 218 and 475 cm<sup>-1</sup> can be assigned to the vibrations of  $S_8$  rings [32,36] and the band at 495 cm<sup>-1</sup> to the vibration of  $S_8$  chain fragments [32,36]. The wide bands at 2800-3000 cm<sup>-1</sup> prove the presence of n-butylamine solvent residue in deposited thin film [37-39]. The Raman spectrum of annealed thin films provides evidence of the polymerization of structure as the concentration of  $As_4S_4$  structural units and  $S_8$  rings decreases while the concentration of  $As_3S_{3/2}$  pyramidal units increases. This polymerization process is accompanied by

the releasing of residual solvent which is shown by the significant decrease in the intensity of the bands at 2800-3000 cm<sup>-1</sup>.

The Raman spectrum in Figure 7 has confirmed the composition of the precipitate to be  $As_2O_3$ , shown, similar to the results reported in [40]. We can predict that in As-rich and even in stoichiometric glass the precipitate could be formed during dissolution of bulk glass by the oxidation of As-As bonds [40]. But the mechanism for the creation of As<sub>2</sub>O<sub>3</sub> precipitate in S-rich compositions is not completely clear yet, since the concentration of As-As bonds is negligible. At the same time, the formation of  $As_2O_3$  is in good agreement with the compositionally dependent loss of As observed by XPS on the surface of SCF in the As-S system, as seen in Table 1. Whereas Chern and Lauks proposed the formation of As-NH<sub>3</sub> compounds through an electrophilic substitution reaction, our results cannot confirm the presence of these fragments in the precipitate. We can only speculate that the weak peaks observed at ~230 cm<sup>-1</sup> and ~415 cm<sup>-1</sup> in Figure 6 are probably associated with these compounds. Further, we believe these units are present throughout the bulk of the SCF. The reason they are not detected with XPS can be in the way SCF is prepared, which includes thermal treatment that causes the evaporation of As-NH3 fragments from the surface region. As seen in Figure 6, after annealing, the Raman band at 415 cm<sup>-1</sup> virtually disappears even from the bulk of SCF. Thus we can expect that the As chemical environment related to As-NH3 also becomes undetectable in the XPS spectra even after the initial thermal treatment at 60 °C. It is reasonable to expect that the evaporation process is much more efficient on the surface of the SCF so that the surface of all studied SCF is deficient in these compounds. In this way, our explanations do not contradict the structural model proposed earlier by Chern and Lauks [17-20].

#### **Conclusions**

The high-resolution XPS measurements show that no organics are directly bonded to the SCF matrix and that As-As bonds are not present in the surface layer of investigated ChG. We conclude that the organic residual in the annealed SCF is connected with the glass matrix through weak ionic bonding with S atoms. Raman spectroscopy confirms that the composition of the precipitate is  $As_2O_3$ , which is in agreement with the observed loss of As during dissolution. The bands associated with the presence of organics and As-amine complexes in virgin SCF are revealed which virtually disappear upon annealing. It is shown that SCFs are photostable, as verified by the lack of change in the optical transmission spectra after bandgap irradiation, due to the observed absence of As-As bonds.

#### Acknowledgements

The authors thank U.S. National Science Foundation, through International Materials Institute for New Functionality in Glass (Grant No. DMR-0844014), for initiating the international collaboration and providing financial support for this work. The group from Austin Peay State University acknowledges financial support from NSF Grant DMR-1409160. Both these NSF grants allowed us to develop an undergraduate research program which contributed to current publication.

#### References

- [1] M. Galili, J. Xu, H. C. H. Mulvad, L. K. Oxenlowe, A. T. Clausen, P. Jeppesen, B. Luther-Davies, S. Madden, A. Rode, D.Y. Choi, M. Pelusi, F. Luan, B. J. Eggleton, Breakthrough switching speed with an all-optical chalcogenide glass chip: 640 Gbit/s demultiplexing, Opt. Express 17 (2009) 2182-2187.
- [2] I.P. Studenyak, M. Kranjcec, M.M. Pop, Urbach absorption edge and disordering processes in As<sub>2</sub>S<sub>3</sub> thin films, J. Non-Cryst. Solids 357 (2011) 3866-3869.
- [3] A. Kovalskiy, M. Vlcek, K. Palka, R. Golovchak, H. Jain, Wavelength Dependence of Photostructural Transformations in As<sub>2</sub>S<sub>3</sub>Thin Films, Phys. Procedia 44 (2013) 75-81.
- [4] V. G. Ta'eed, N. J. Baker, L. Fu, K. Finsterbusch, M. R. E. Lamont, D. J. Moss, H. C. Nguyen, B. J. Eggleton, D.Y. Choi, S. Madden, B. Luther-Davies, Ultrafast all-optical chalcogenide glass photonic circuits, Opt. Express 15 (2007) 9205-9221.
- [5] K. Tanaka, K. Shimakawa, *Amorphous Chalcogenide Semiconductors and Related Materials*. Springer Science+Business Media, New York (2011).
- [6] A. Zakery, S. R. Elliott. Optical Nonlinearities in Chalcogenide Glasses and their Applications. Springer-Verlag Berlin Heidelberg (2007).
- [7] D.Y. Choi, A. Wade, S. Madden, R. Wang, D. Bulla, B. Luther-Davies, Photo-induced and Thermal Annealing of Chalcogenide Films for Waveguide Fabrication, Phys. Procedia, 48 (2013) 196-205.
- [8] A. Kovalskiy, J. Cech, M. Vlcek, C. M. Waits, M. Dubey, W. R. Heffner, H. Jain, "Chalcogenide glass e-beam and photoresists for ultrathin grayscale patterning," J. Micro/Nanolith. MEMS MEOMS 8(4), (Oct-Dec 2009) 043012.
- [9] J. Hu, V. Tarasov, N. Carlie, N.N. Feng, L. Petit, A. Agarwal, K. Richardson, L. Kimerling, Si-CMOS-compatible lift-off fabrication of low-loss planar chalcogenide waveguides, Opt. Express 15 (2007) 11798-11807.
- [10] L. Li, Y. Zou, H. Lin, J. Hu, X. Sun, N. Feng, S. Danto, K. Richardson, T. Gu, M. Haney, A Fully-integrated Flexible Photonic Platform for Chip-to-chip Optical Interconnects, J. Lightwave Technol. 31 (2013) 4080-4086.
- [11] L. Li, H. Lin, S. Qiao, Y. Zou, S. Danto, K. Richardson, J. D. Musgraves, N. Lu, J. Hu, Integrated flexible chalcogenide glass photonic devices, Nature Photon. 8 (2014) 643-649.
- [12] C. Tsay, Y. Zha, C. B. Arnold, Solution-processed chalcogenide glass for integrated single-mode mid-infrared waveguides, Opt. Express 18 (2010) 26744-26753.
- [13] M. Krbal, T. Wagner, T. Kohoutek, P. Nemec, J. Orava, M. Frumar, The comparison of Ag-As<sub>33</sub>S<sub>67</sub> films prepared by thermal evaporation (TE), spin-coating (SC) and a pulsed laser deposition (PLD), J. Phys. Chem. Solids 68 (2007) 953-957.
- [14] J.M. Gonzales-Leal, M. Stuchlik, M. Vlcek, R. Jimenez-Garay, E. Marquez, Influence of the deposition technique on the structural and optical properties of amorphous As-S films, Appl. Surf. Sci. 246 (2005) 348-355.
- [15] L. Tichy, H. Ticha, P. Nagels, R. Callaerts,
- Photoinduced changes in the short wavelength optical absorption edge of a-As<sub>2</sub>S<sub>3</sub> and a-As<sub>2</sub>Se<sub>3</sub> thin amorphous films, Mater. Lett. 36 (1998) 294-298.
- [16] S. Shtutina, M. Klebanov, V. Lyubin, S. Rosenwaks, V. Volterra, Photoinduced phenomena in spin-coated vitreous As<sub>2</sub>S<sub>3</sub> and AsSe films, Thin Solid Films 261 (1995) 263-265.
- [17] G. C. Chern and I. Lauks, Spincoated amorphous chalcogenide films, J. Appl. Phys. 53 (1982) 6979-6982.

- [18] G. C. Chern and I. Lauks, Spin coated amorphous chalcogenide films: Structural characterization, J. Appl. Phys. 54 (1983) 2701-2705.
- [19] G. C. Chern and I. Lauks, Spin-coated Amorphous Chalcogenide Films: Photoinduced Effects, Thin Solid Films, 123 (1985) 289-296.
- [20] G. C. Chern and I. Lauks, Spin coated amorphous chalcogenide films: Thermal properties, J. Appl. Phys. 54 (1983) 4596-4601.
- [21] R. Golovchak, O. Shpotyuk, S. Kozyukhin, A. Kovalskiy, A.C. Miller, H. Jain, Structural paradigm of Se-rich Ge-Se glasses by high-resolution X-ray photoelectron spectroscopy, J. Appl. Phys. 105 (2009) 103704-103711.
- [22]R. Golovchak, O. Shpotyuk, M. Iovu, A. Kovalskiy, H. Jain, Topology and chemical order in As<sub>x</sub>Ge<sub>x</sub>Se<sub>1-2x</sub> glasses: a high-resolution X-ray photoelectron spectroscopy study, J. Non-Cryst. Solids 357 (2011) 3454-3460.
- [23] S. Kozyukhin, R. Golovchak, A. Kovalskiy, O. Shpotyuk, H. Jain, Valence band structure of binary chalcogenide vitreous semiconductors by high-resolution XPS, Semiconductors 45 (2011) 423-426.
- [24] R. Golovchak, O. Shpotyuk, J. Mccloy, B. Riley, C. Windisch, S. Sundaram, A. Kovalskiy, Structural model of homogeneous As–S glasses derived from Raman spectroscopy and high-resolution XPS, Philos. Mag. 90 (2010) 4489-4501.
- [25] A. Kovalskiy, R. Golovchak, M. Vlcek, H. Jain, Electronic and atomic structure of amorphous thin films with high-resolution XPS: Examples of applications & limitations, J. Non-Cryst. Solids 377 (2013) 155-158.
- [26] A. Kovalskiy, M. Vlcek, H. Jain, A. Fiserova, C. M. Waits, M. Dubey, Development of chalcogenide glass photoresists for grayscale lithography, J. Non-Cryst. Solids 352 (2006) 589-594.
- [27] A. Kovalskiy, J. R. Neilson, A. C. Miller, F. C. Miller, M. Vlcek, H. Jain, Comparative study of electron-and photo-induced structural transformations on the surface of As<sub>35</sub>S<sub>65</sub> amorphous thin films, Thin Solid Films, 516 (2008) 7511-7518.
- [28] J. M. Conny, C. J. Powell, Standard test data for estimating peak parameter errors in x-ray photoelectron spectroscopy III. Errors with different curve-fitting approaches, Surf. Interface Anal. 29 (2000) 856-872.
- [29] A. Kovalskiy, H. Jain, M. Mitkova, Evolution of chemical structure during silver photodiffusion into chalcogenide glass thin films, J. Non-Cryst. Solids 355 (2009) 1924-1929.
- [30] A. Kovalskiy, J. Cech, C. L. Tan, W. R. Heffner, E. Miller, C. M. Waits, M. Dubey, W. Churaman, M. Vlcek, H. Jain, Chalcogenide glass thin film resists for grayscale lithography, Proc. Of SPIE Vol. 7273, 72734A (2009).
- [31] R. Ston, M. Vlcek, H. Jain, Structure and photoinduced changes in bulk and films of As—Ge–S system, J. Non-Cryst. Solids 236 (2003) 220-225.
- [32] M. Pisarcik, L. Koudelka, Raman spectra and structure of Ge-As-S glasses in the S-rich region, Mater. Chem. 7 (1982) 499.
- [33] R. Holomb, V. Mitsa, O. Petrachenkov, M. Veres, A. Stronski and M. Vlcek, Comparison of structural transformations in bulk and as-evaporated optical media under action of polychromatic or photon-energy dependent monochromatic illumination, Phys. Status Solidi 8 (2011) 2705-2708.
- [34] I. Ivan, M. Veres, I. Pocsik and S. Kokenyes, Structural and optical changes in As2S3 thin films induced by light ion irradiation, Phys. Status Solidi 201 (2004) 3193-3199.

- [35] D. Arsova, E. Skordeva, D. Nesheva, E. Vateva, A. Perakis, and C. Raptis, A comparative raman study of the local structure in (Ge2S3)<sub>x</sub>(As2S3)<sub>1-x</sub> and (GeS2)<sub>x</sub>(As2S3)<sub>1-x</sub> glasses, Glass Phys. Chem. 26 (2000) 247-251.
- [36] Z. Cernosek, J. Holubova, E. Cernoskova, A. Ruzicka, Sulfur a new information on this seemingly well-known element, J. Non-Cryst. Solids 1 (2009) 38-42.
- [37] S. A. Zenkin, S. B. Mamedov, M.D. Mikhailov, E.Yu. Turkina, I.Yu. Yusupov, Mechanism for interaction of amine solutions with monolithic glasses and amorphous films in the As-S system, Glass Phys. Chem. 23 (1997) 393.
- [38] Y. Zha, S. Fingerman, S. J. Cantrell and C. B. Arnold, Pore formation and removal in solution-processed amorphous arsenic sulfide films, J. Non-Cryst. Solids 369 (2013) 11-16.
- [39] T. A. Guiton, C. Pantano, Solution/gelation of arsenic trisulfide in amine solvents, Chem. Mater. 1 (1989) 558-563.
- [40] S. Gilliam, C. Merrow, Raman spectroscopy of arsenolite: crystalline cubic As<sub>4</sub>O<sub>6</sub>, J. Solid State Chem. 173 (2003) 54-58.

## **Figure Captions**

- Figure 1: As 3d XPS core level spectra of virgin (a)  $As_{30}S_{70}$ , (b)  $As_{35}S_{65}$  and (c)  $As_{40}S_{60}$  SCF.
- Figure 2: S 2p XPS core level spectra of virgin (a) As<sub>30</sub>S<sub>70</sub>, (b) As<sub>35</sub>S<sub>65</sub> and (c) As<sub>40</sub>S<sub>60</sub> SCF.
- Figure 3: As 3d XPS core level spectra of  $As_{35}S_{65}$  (a) annealed and (b) exposed SCF.
- Figure 4: S 2p XPS core level spectra of As<sub>35</sub>S<sub>65</sub> (a) annealed and (b) exposed SCF.
- Figure 5: Optical transmission spectra before and after irradiation of (a)  $As_{30}S_{70}$  and (b)  $As_{40}S_{60}$  SCF.
- Figure 6: Raman spectrum of virgin and annealed As<sub>30</sub>S<sub>70</sub> SCF.
- Figure 7: Raman spectrum of solution precipitate of As<sub>35</sub>S<sub>65</sub> solution.

## **Highlights**

- As-S spin-coated chalcogenide thin films with different As/S were fabricated
- XPS measurements support the cluster-like structure of spin-coated films
- As<sub>2</sub>O<sub>3</sub> was confirmed as the composition of precipitate formed during dissolution
- Lack of As-As bonds explains the observed photostability of the thin films

Table 1: Numerical parameters of As  $3d_{5/2}$  and  $S2p_{3/2}$  XPS core level spectra.

			S	- <b>As-(S)</b> <sub>2</sub>		A	ls <b>-S</b> -As		Å	S- <b>S</b> -As			S-			S- <b>S</b> -S	
Composition	As %	S %	BE (eV)	FWHM (eV)	A (%)	BE (eV)	FWHM (eV)	A (%)	BE (eV)	FWHM (eV)	A (%)	BE (eV)	FWHM (eV)	A (%)	BE (eV)	FWHM (eV)	A (%)
$As_{30}S_{70}$	30	70	43.05	0.83	100	162.20	0.86	54	162.95	0.98	28	161.15	0.98	9	163.75	0.71	9
$As_{35}S_{65}$	32	68	43.05	0.78	100	162.10	0.84	65	162.90	0.90	21	161.05	0.98	10	163.70	0.64	4
Exposed As <sub>35</sub> S <sub>65</sub>	32	68	43.20	0.74	100	162.30	0.80	58	163.00	0.98	37	161.15	0.76	3	163.80	0.44	2
Annealed As <sub>35</sub> S <sub>65</sub>	33	67	43.05	0.74	100	162.15	0.80	73	162.90	0.76	15	161.25	0.98	8	163.60	0.98	4
$As_{40}S_{60}$	35	65	43.20	0.78	100	162.25	0.83	78	163.00	0.82	12	161.20	0.82	10			

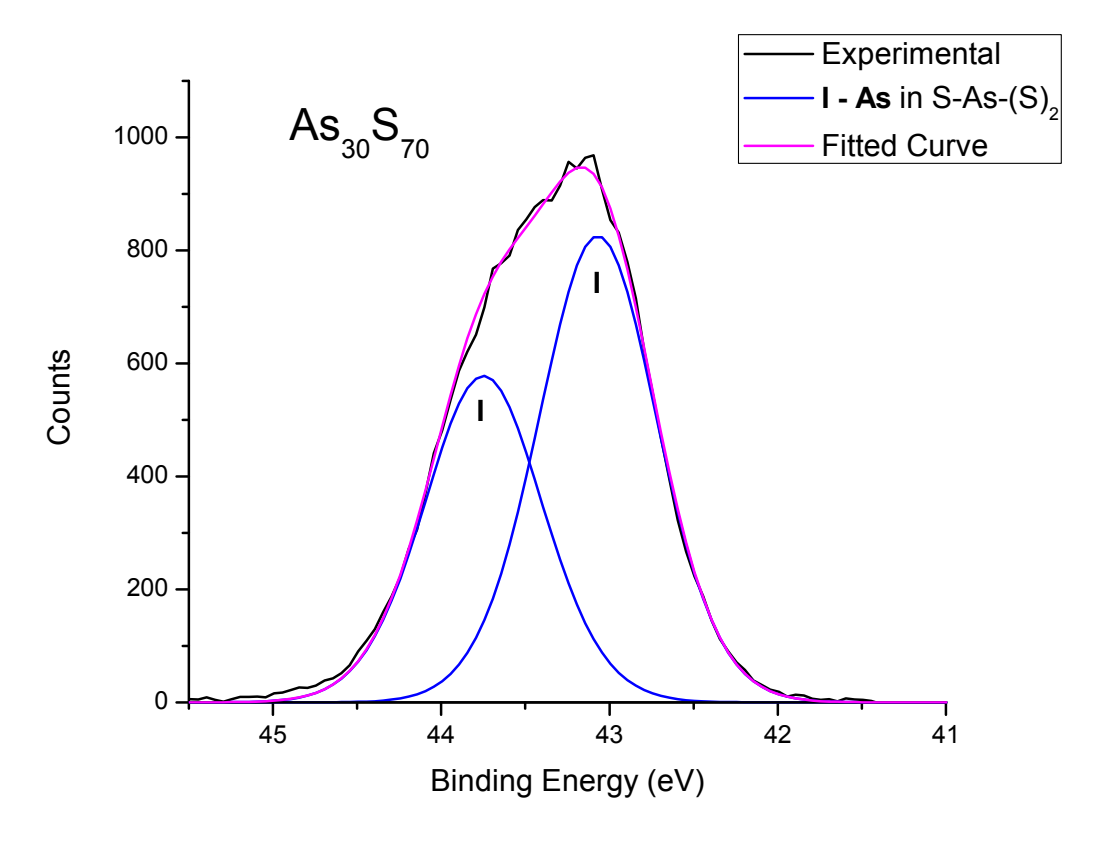


Figure 1a

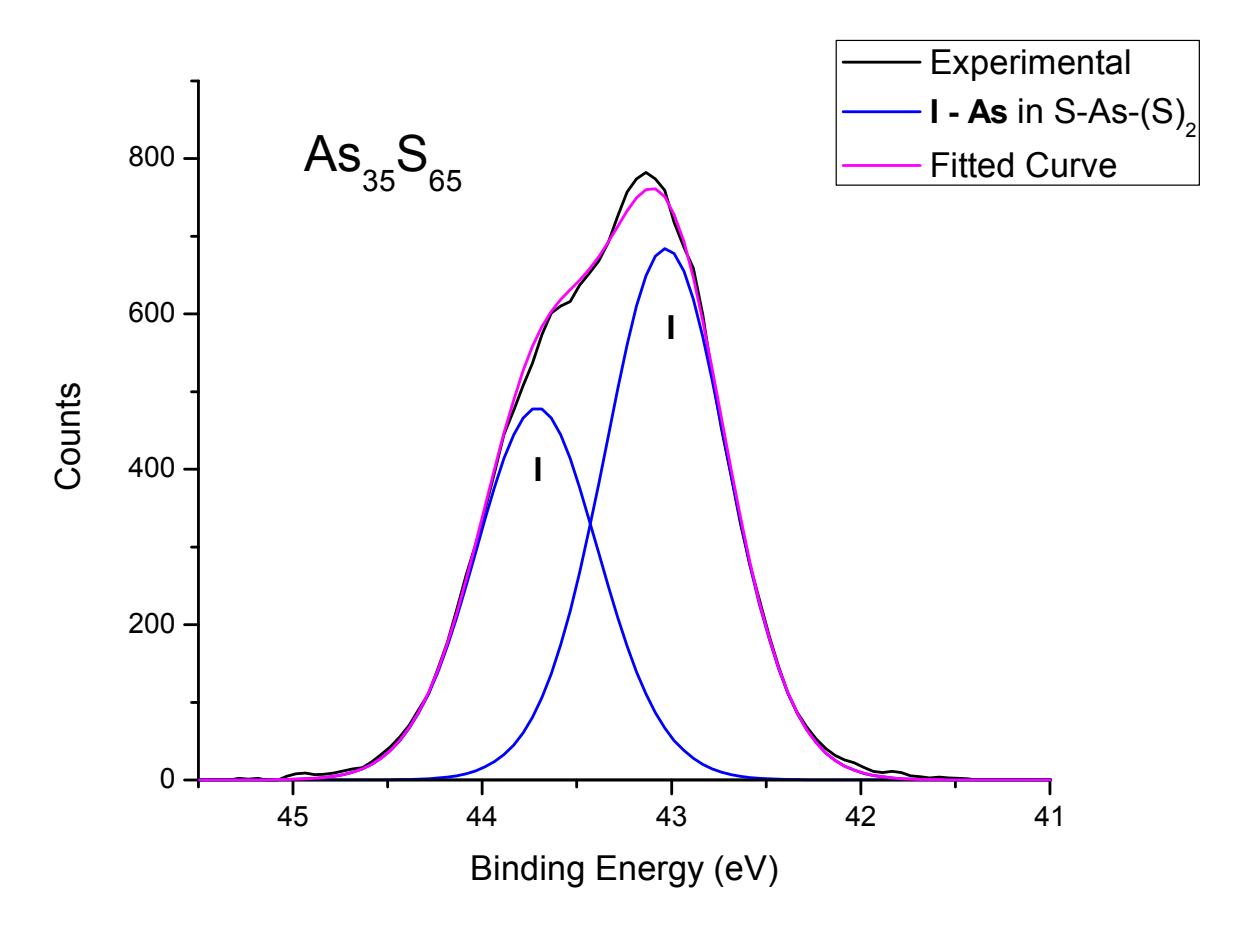


Figure 1b

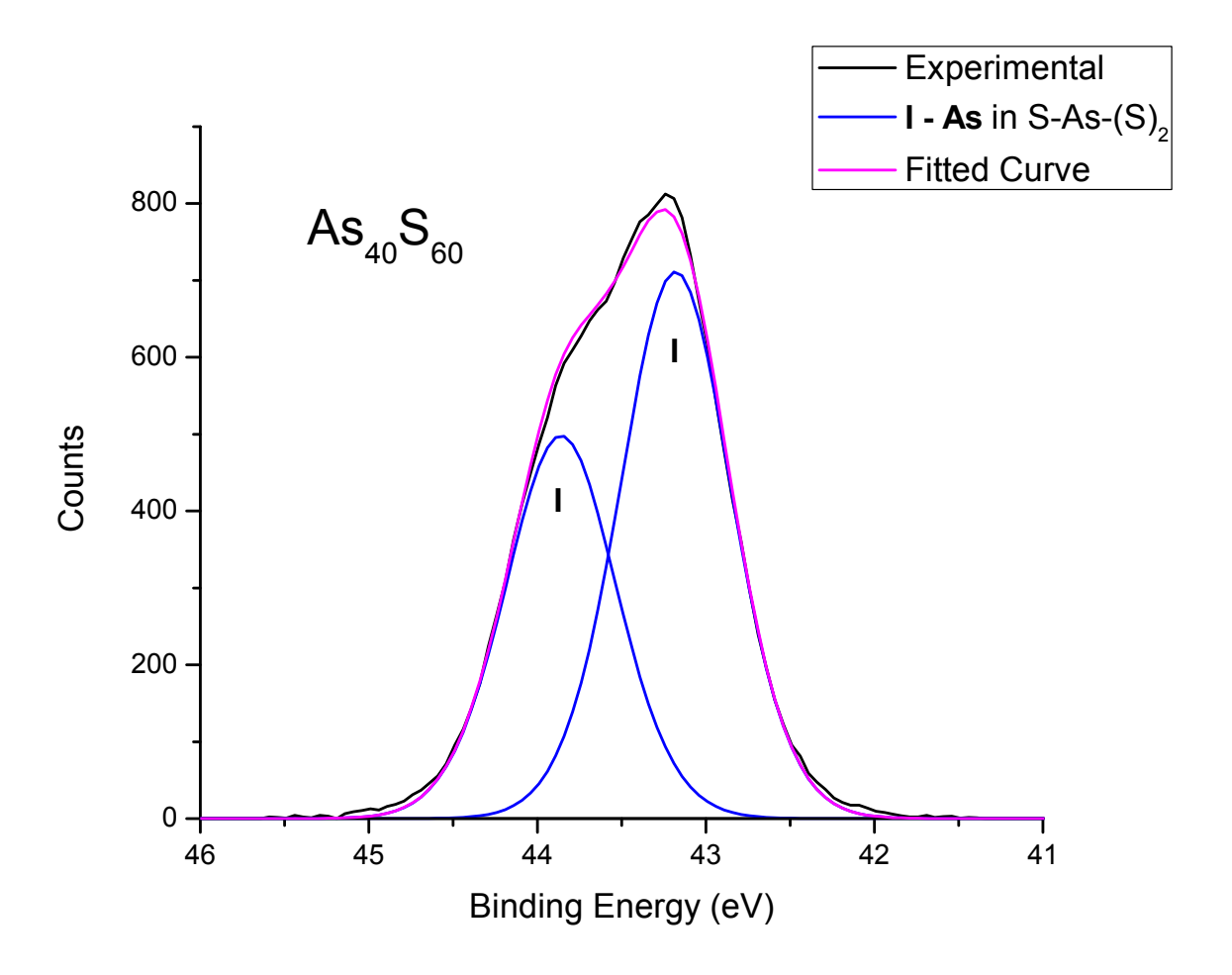


Figure 1c

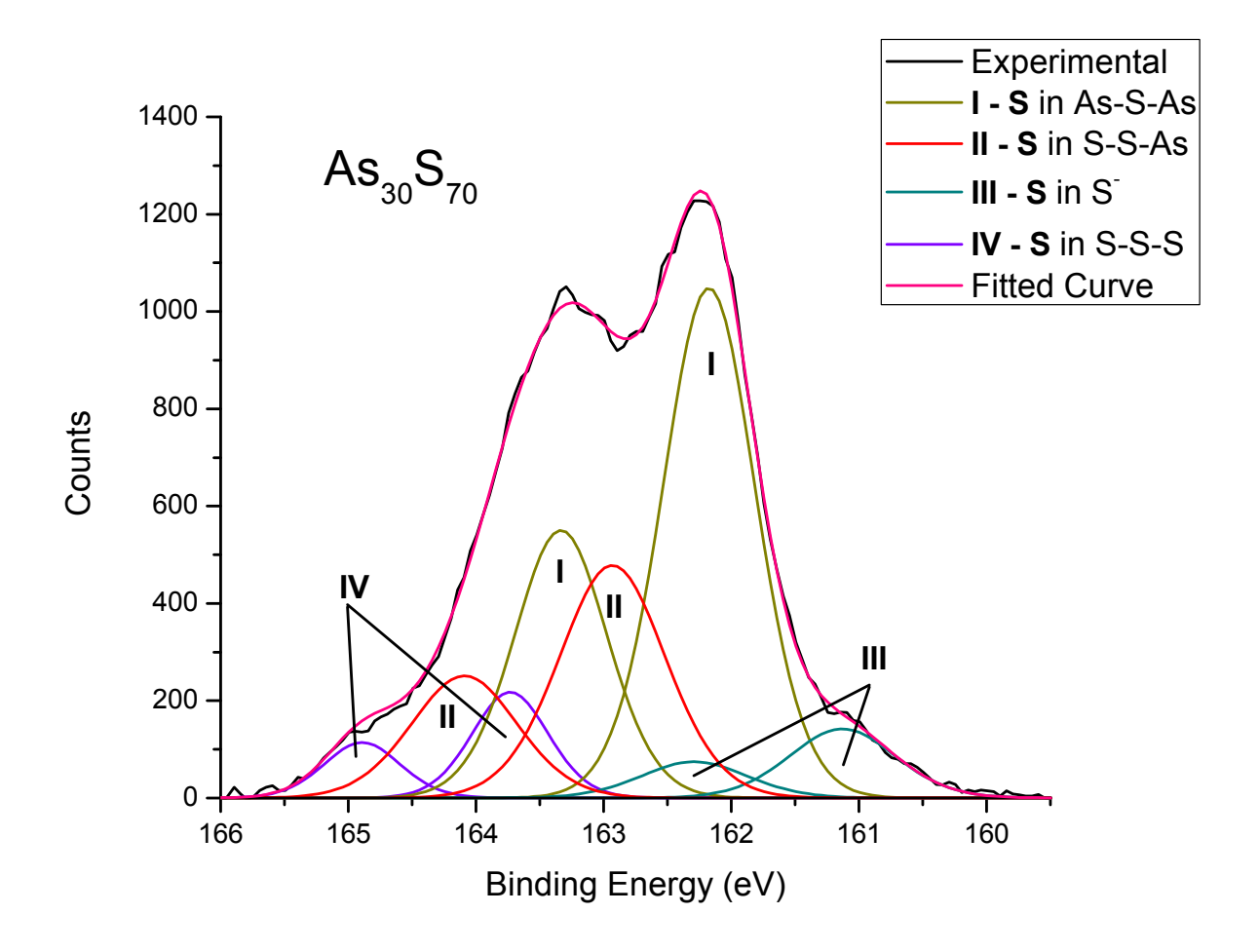


Figure 2a

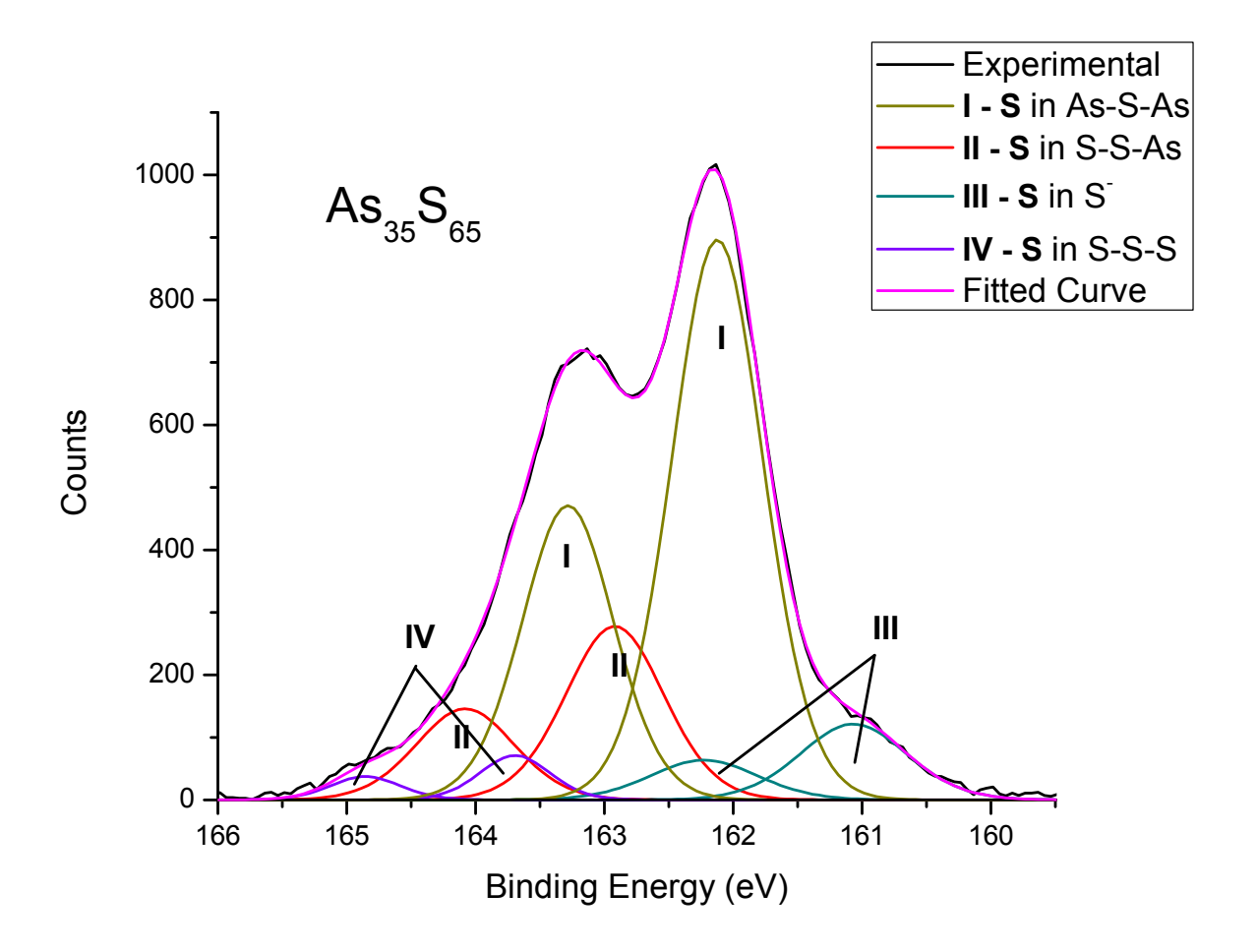


Figure 2b

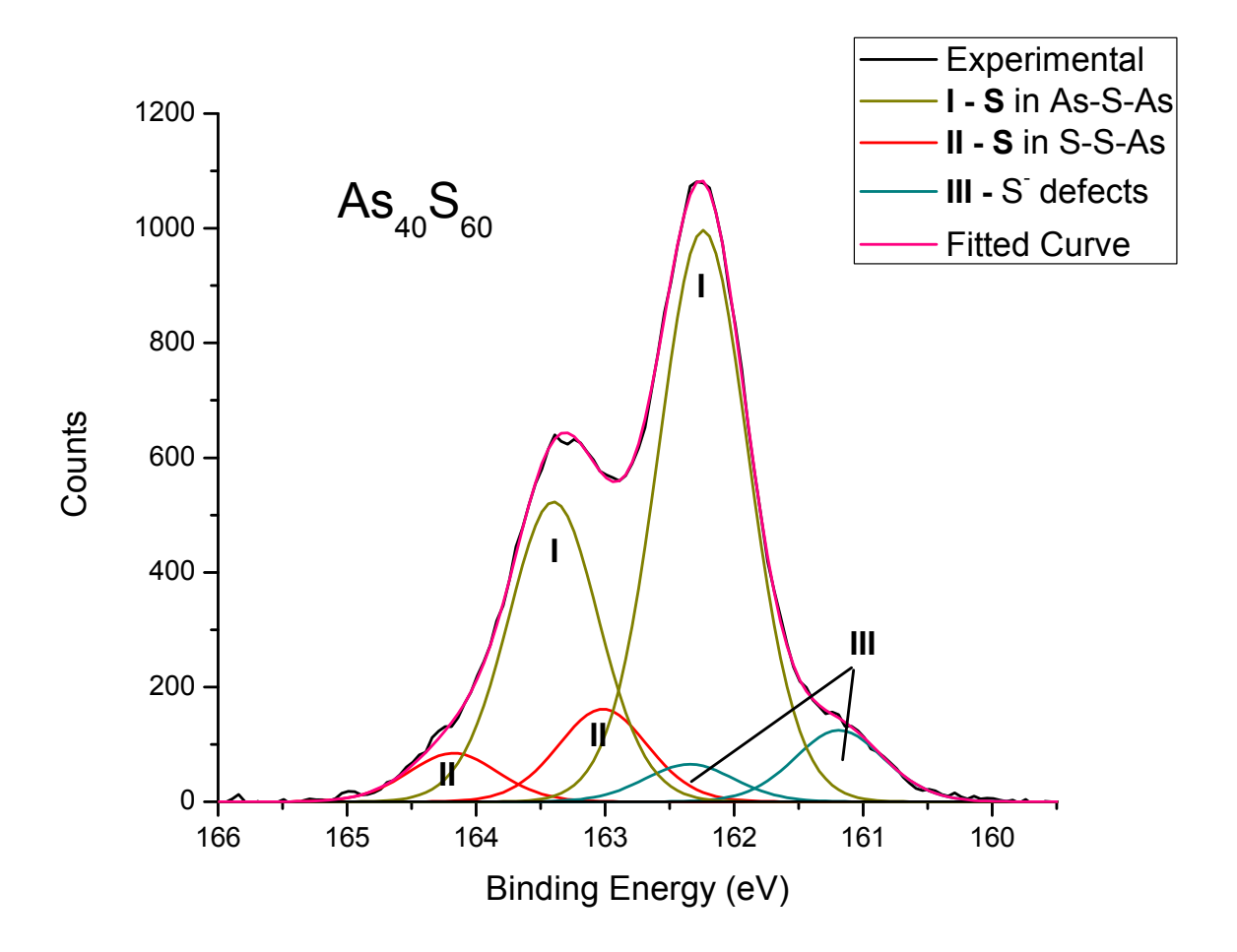


Figure 2c

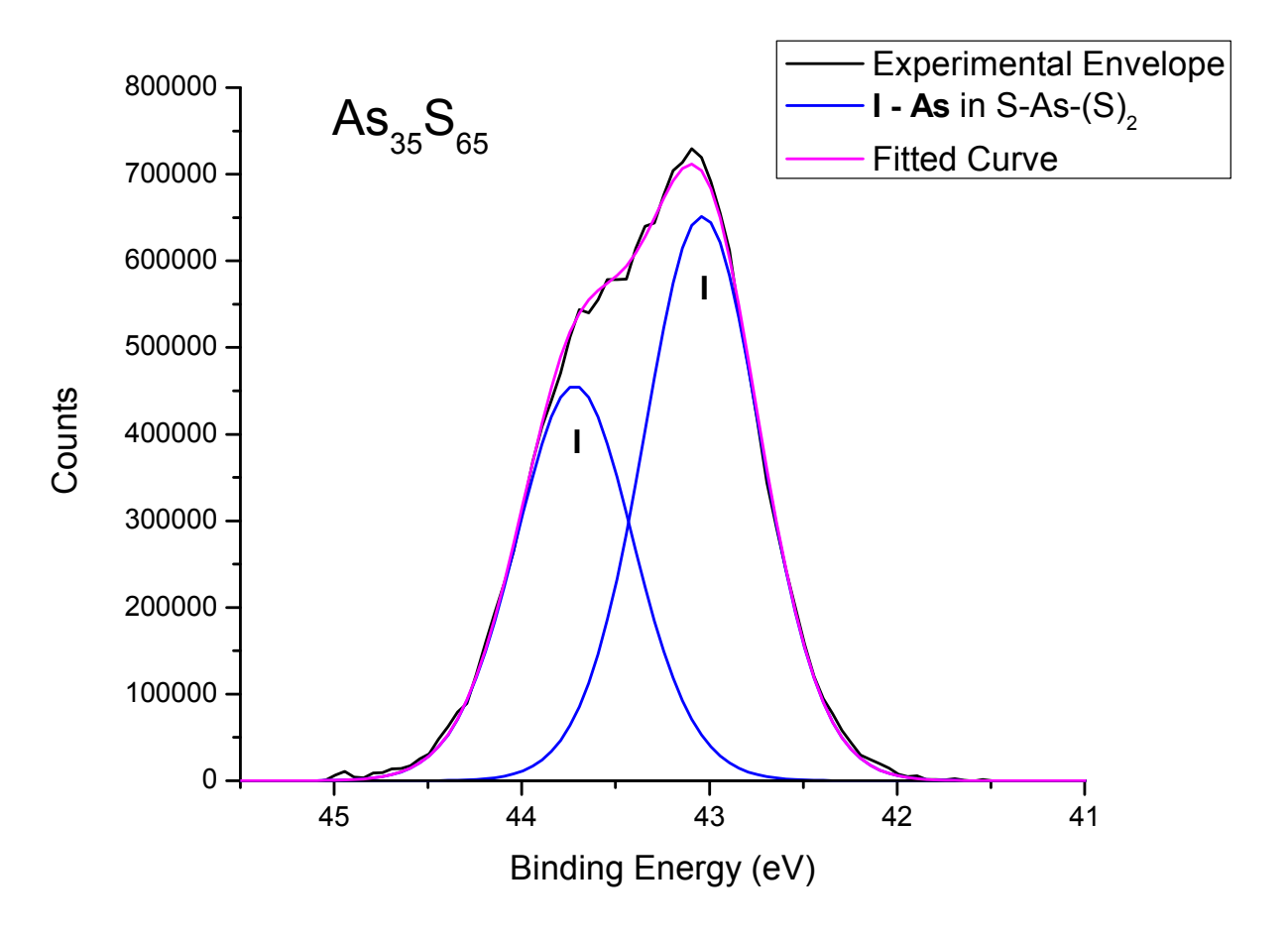


Figure 3a

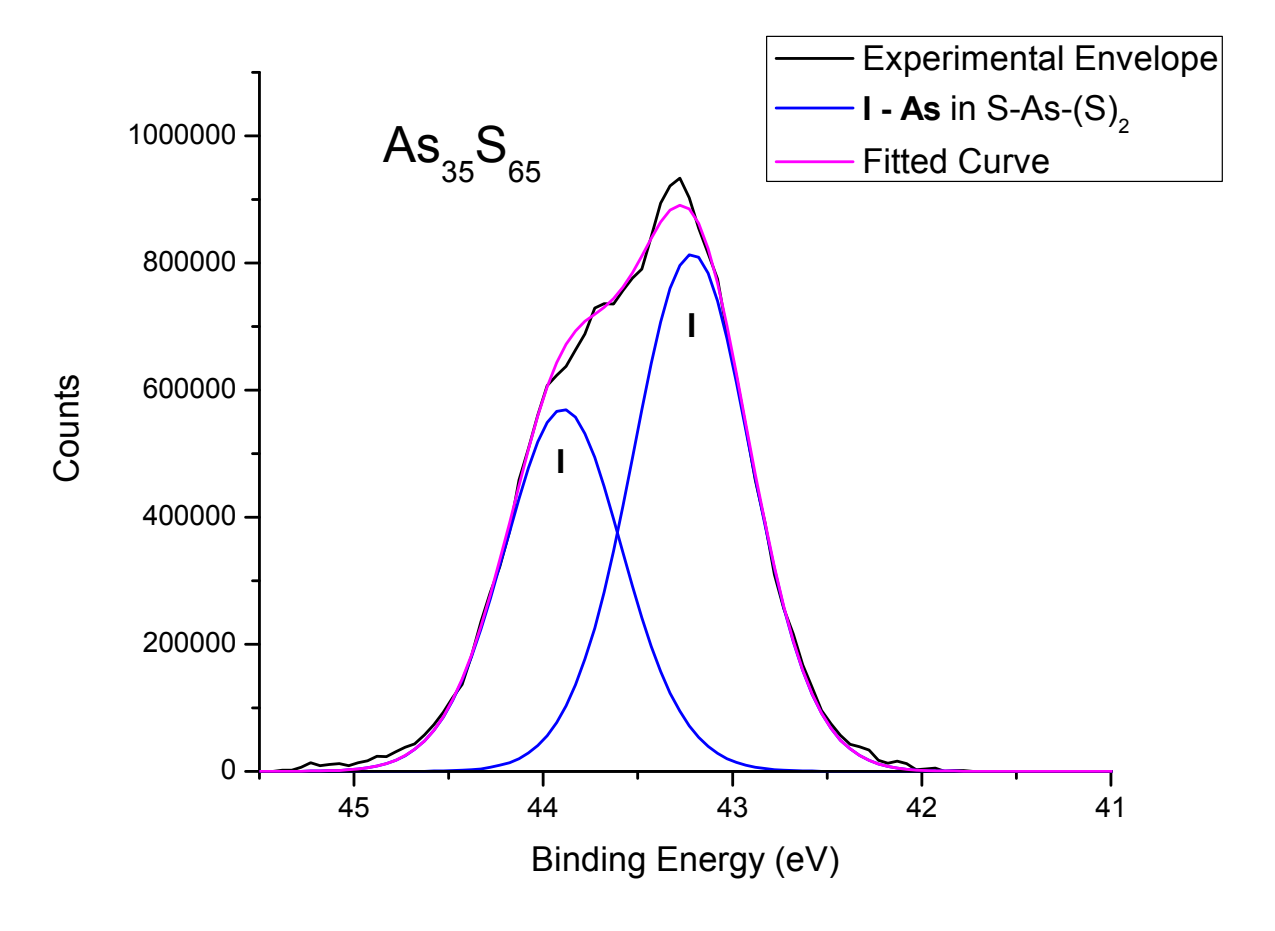


Figure 3b

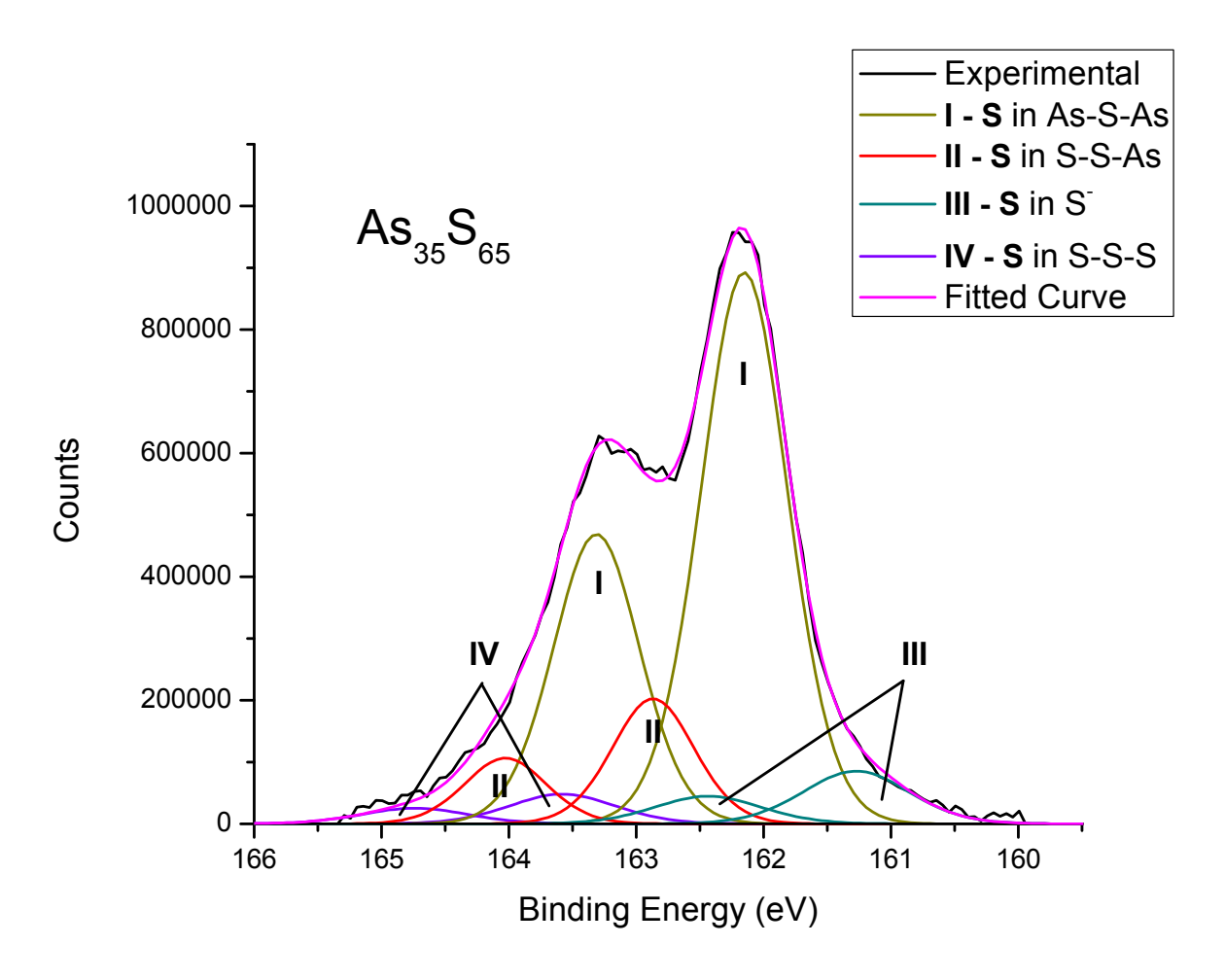


Figure 4a

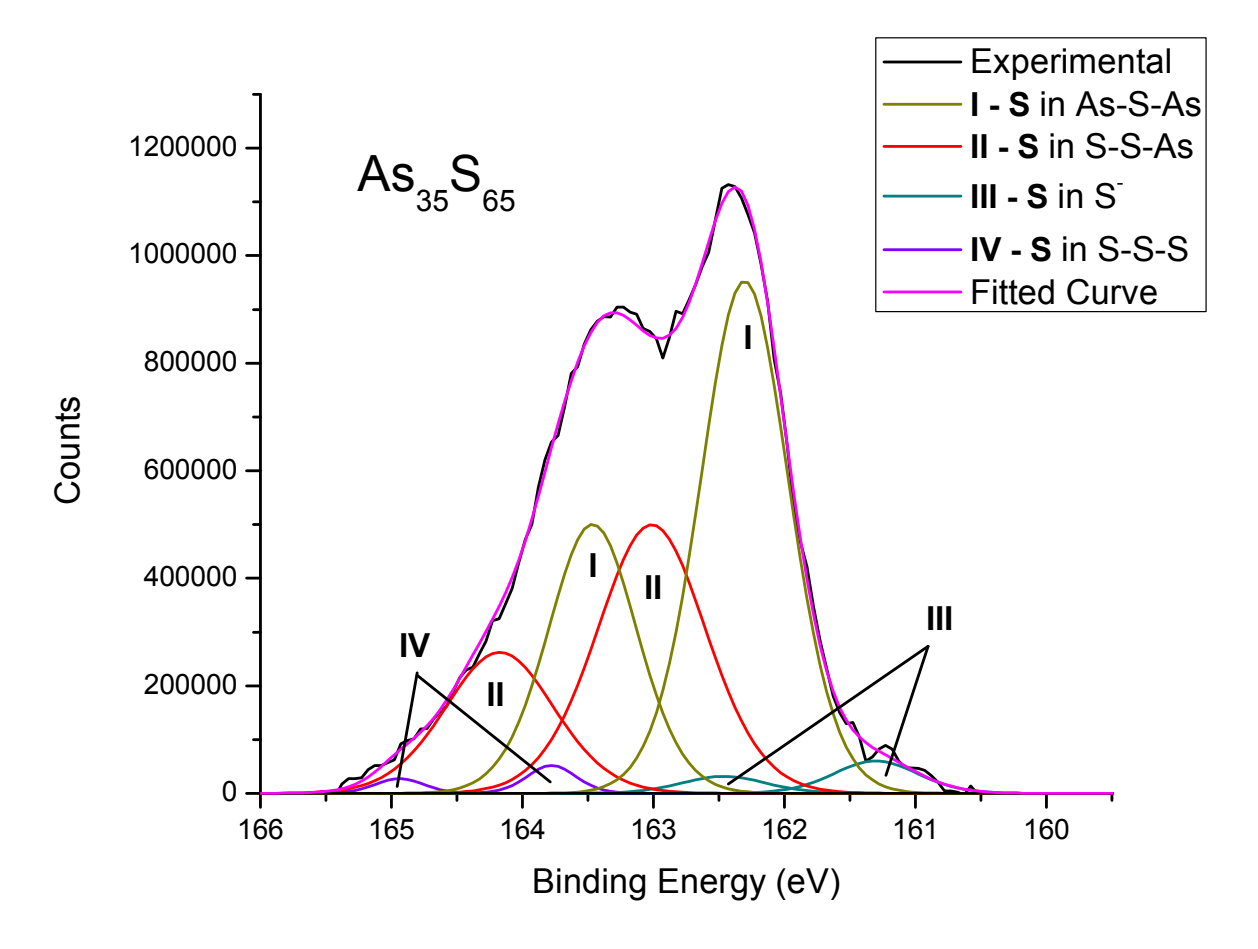


Figure 4b

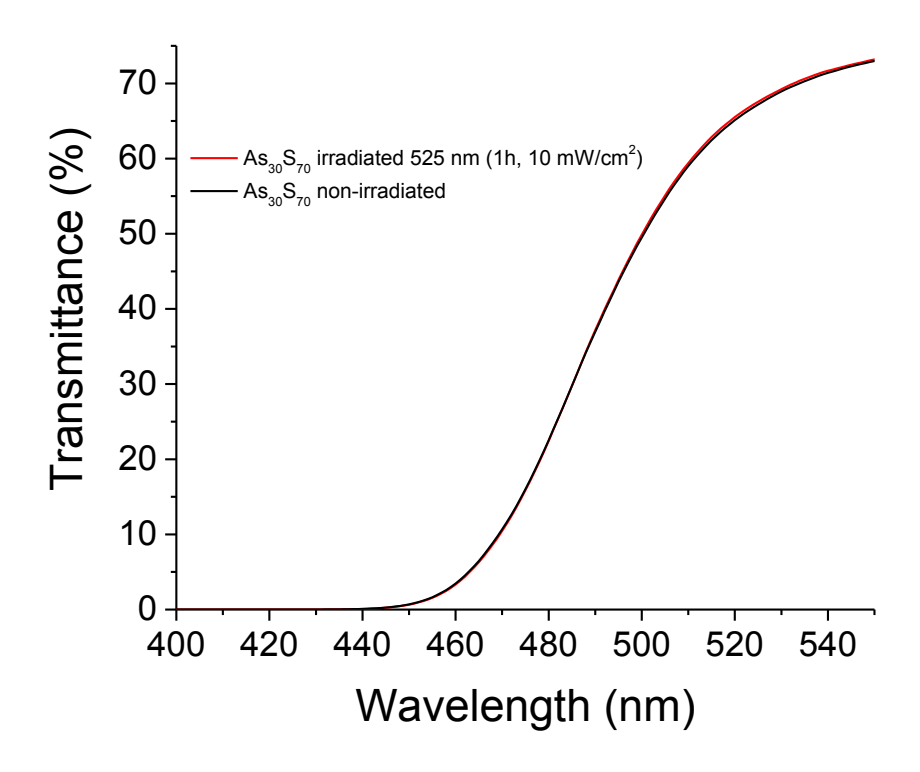


Figure 5a

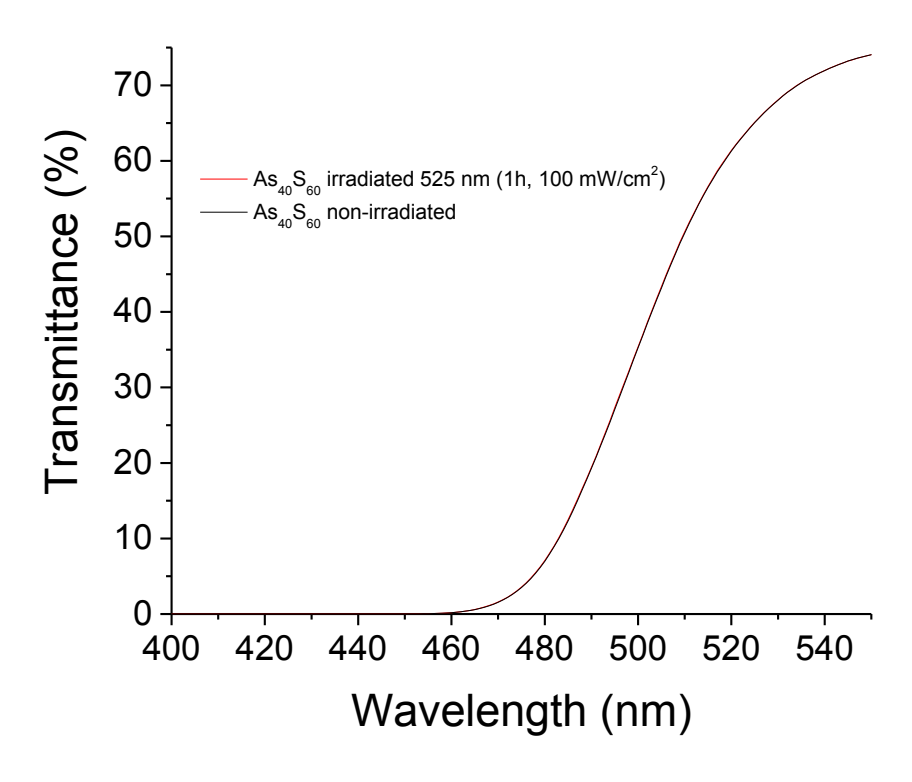


Figure 5b

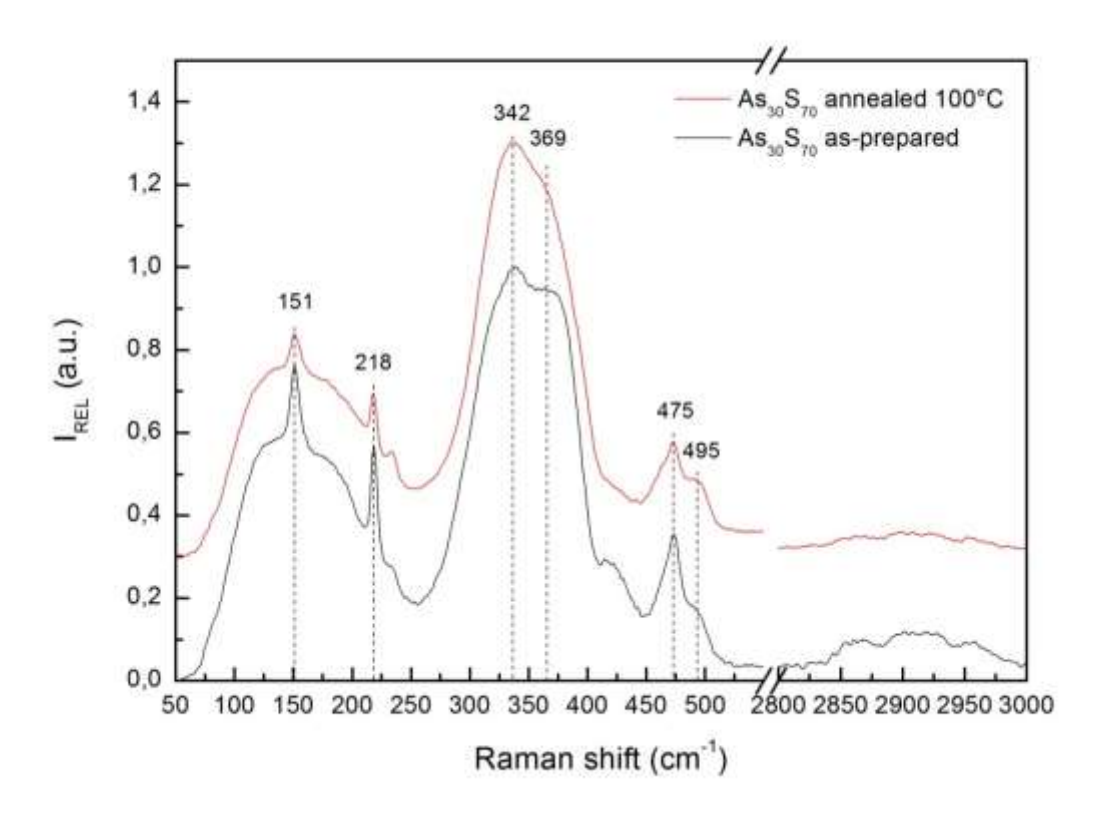


Figure 6

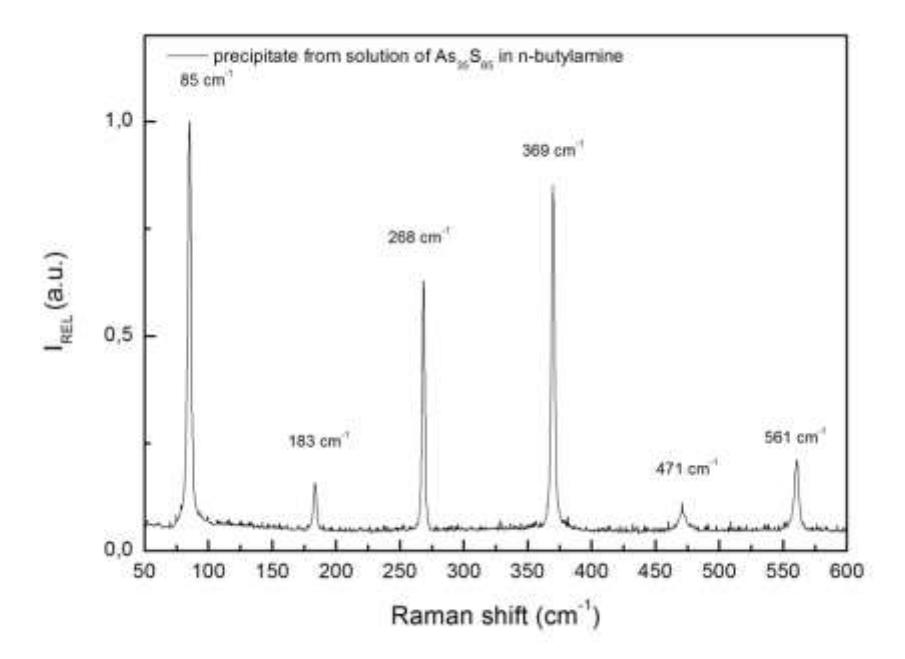


Figure 7